Portugaliae Electrochimica Acta 2010, 28(2), 95-112

DOI: 10.4152/pea.201002095

PORTUGALIAE ELECTROCHIMICA ACTA
ISSN 1647-1571

Inhibition of Uniform and Pitting Corrosion Processes of Al Induced by SCN^- anions – Part I. Effect of Glycine

Mohammed A. Amin,[*] Q. Mohsen, Gaber A.M. Mersal

Materials and Corrosion Lab, Faculty of Science, Chemistry Department, Taif University, 888 Hawiya, KSA

Received 17 March 2010; accepted 11 May 2010

Abstract

As a first step towards inhibition of uniform and pitting corrosion processes of Al in SCN^- solutions, glycine (Gly) was used. Full immersion tests, using inductively coupled plasma atomic emission spectroscopy (ICP-AES) method of chemical analysis were used to monitor rates of corrosion. The results obtained from the ICP method have been verified by electrochemical assays based on linear and cyclic polarization measurements. Monitoring the open circuit potential (OCP) of the system as a function of immersion time and Gly concentration was also carried out. SEM and EDX examinations of the electrode surface revealed the adsorption of Gly molecule on the surface. Results showed that the presence of Gly in aggressive SCN^- solutions decreased the corrosion and passive currents and shifted the pitting potential to more noble values. Thus Gly inhibited uniform and pitting corrosion processes. The inhibition efficiency of Gly enhanced with its concentration. The potential of zero charge (PZC) of the Al electrode has been studied in 0.04 M KSCN solutions without and with Gly and the mechanism of adsorption is discussed. The adsorption of Gly precluded significant adsorption of the aggressive SCN^- anions, and hence the corrosion rate was diminished.

Keywords: aluminum, uniform corrosion; pitting corrosion; corrosion inhibition; SCN^- anions; glycine.

Introduction

Aluminum is an important material for use in many applications, such as for automobiles, aviation, household appliances, containers, and electronic devices [1–3], owing to its many favorable characteristics, including its good electrical

[*] Corresponding author. Permanent address: Department of Chemistry, Faculty of Science, Ain Shams University, 11566 Abbassia, Cairo, Egypt. E-mail address: maaismail@yahoo.com

and thermal conductivities, low density, high ductility, and good corrosion resistance.

The resistance of aluminum against corrosion in aqueous media can be attributed to a rapidly formed surface oxide film. However, the presence of aggressive ions like chloride creates extensive localized attack. Our previous studies [4-8] have shown that aluminum and some of its alloys also suffer from localized corrosion due to the aggressive attack of ClO_4^- and SCN^- anions.

Generally, localized corrosion can be prevented by the action of adsorptive inhibitors which prevent the adsorption of the aggressive anions or by the formation of a more resistant oxide film on the metal surface [9]. Chromates are recognized as being very efficient to inhibit the corrosion of aluminum and aluminum alloys. The action is linked, firstly to the formation of an insoluble chromium oxide Cr_2O_3, which strengthens the alumina layer, and secondly to the incorporation of chromate ions in the alumina film, which prevent pitting corrosion through their ability to repair defects in the oxide film [6,10-14].

Literature survey showed that a number of organic compounds were described as aluminum corrosion inhibitors in a variety of media [15-21]. Other organic compounds were used in our lab as inhibitors for corrosion of aluminum and some of its alloys in acidic, neutral and weakly alkaline solutions [22-29]. The majority of these organic inhibitors are toxic. The toxicity of these organic compounds and chromates has led to interest in the use of more environmentally acceptable treatment. Amino acids are biodegradable and might accommodate at least some of the environmental restrictions.

The present work reports on the results obtained in the study of glycine (Gly) as a safe-inhibitor for Al corrosion processes (uniform and pitting) in KSCN solutions at 25 ^oC. For this purpose, chemical (ICP-AES) and electrochemical (linear and cyclic polarization) methods were used, complemented with SEM and EDX examinations of the electrode surface. We are considering this work as a starting point to protect Al against corrosion in the aggressive SCN^- solutions. Glycine, the simplest amino acid, will be studied first. A new glycine derivative was synthesized in our lab and will be described and fully discussed in a further complementary paper.

Experimental

The working electrode employed here was made of pure Al (99.98%) provided by the Egyptian Aluminum Company (EAC). The Al electrode was used in the as-received condition. The investigated electrode was cut as a cylindrical rod, welded with Cu-wire for electrical connection and mounted into glass tubes of appropriate diameter using Araldite to offer an active flat disc shaped surface of (0.50 cm^2) geometric area for the working electrode, to contact the test solution. Prior to each experiment, the electrode surface was wet polished with silicon carbide from 220 to 500 grits, degreased with acetone and, finally, rinsed with distilled water.

All experiments (either chemical or electrochemical) were carried out in 0.04 M KSCN solutions without and with various concentrations (10^{-5} – 5×10^{-3} M) of Gly. All solutions were freshly prepared from analytical grade chemical reagents using doubly distilled water and were used without further purification. For each run, a freshly prepared solution as well as a cleaned set of electrodes was used. Each run was carried out in aerated stagnant solutions at the required temperature (±1 ºC), using a water thermostat.

Full immersion tests were performed in accordance with the ASTM-G31 standard [30]. Exposure times between 1.0 and 30 days were used. Corrosion rates were monitored in 0.04 M KSCN solutions without and with various concentrations of Gly as a function of the immersion time (1-30 days) at 25 ± 1 ^{o}C using inductively coupled plasma atomic emission spectroscopy (ICP-AES) method of chemical analysis. After these immersion essays, micro-structural features of some of the exposed samples were analyzed by EDX and SEM examinations using a Jeol-Jem-1200 EX II electron microscope equipped with a Traktor TN-2000 energy dispersive spectrometer.

In the ICP method, the Al^{3+} ions concentration was determined using Perkin-Elmer Optima 2100 Dual View inductively coupled plasma atomic emission spectrometry (ICP-AES) instrument connected with AS 93 Plus autosampler. The 40-MHz free-running generator was operated at a forward power of 1.3 kW; the outer, intermediate and Ar carrier gas flow rates were 15.0, 0.2 and 0.8 L/min, respectively. The carrier gas flow rate was optimized to obtain maximum signal-to-background ratios. In all experiments, the measured samples were nebulized downstream to the plasma by the autosampler and the concentrations were automatically determined using the standard calibration graph. The system adjusted to measure the samples in triplicates and the relative standard deviation was calculated. The RSD was < 2 % and the correlation coefficient was > 0.99998.

Electrochemical experiments were performed in a 100 mL volume Pyrex glass cell using Pt wire and a saturated calomel electrode (SCE) as auxiliary and reference electrodes, respectively. The SCE was connected via a Luggin capillary, the tip of which was very close to the surface of the working electrode to minimize the IR drop. All potentials given in this paper are referred to this reference electrode.

Electrochemical measurements were performed using Autolab frequency response analyzer (FRA) coupled to an Autolab Potentiostat/Galvanostat (PGSTAT30) with FRA2 module connected to a personal computer**.**

Linear polarization technique has been used to evaluate the degree of protection against uniform corrosion processes supplied by Gly, as well as to obtain information about the mechanism of the inhibition process.

On the other hand, pitting corrosion inhibition degree has been evaluated in terms of both nucleation of pits and growth of pre-existing pits, using cyclic polarization technique. Measurements were carried out by sweeping linearly the potential from the starting potential, -2000 mV (SCE), into the positive direction, at a scan rate of 0.50 mV s^{-1} up to the end potential, +2000 mV (SCE), (linear polarization) and then reversed with the same scan rate till forming a well-

defined hysteresis loop (cyclic polarization). The stabilization period prior to collecting data was 12 h. The open circuit potential of the working electrode was measured as a function of time during this stabilization time. This time was quite sufficient to reach a quasi-stationary value for the open circuit potential.
Complex-plane impedance plots were also recorded for Al in 0.04 M KSCN solutions without and with $5x10^{-3}$ M Gly as a function of potential, and a plot of capacitance vs. potential plot was constructed. The aim is to study the potential of zero charge (PZC) of Al in these solutions in order to gain more information regarding the electrostatic adsorption of Gly. Impedance measurements were carried out using AC signals of amplitude 5.0 mV peak to peak at the open circuit potential in the frequency range 100 kHz–1.0 mHz. Capacitance values were evaluated based on the equivalent circuit presented in our previous study [8].
Other Al samples were exposed to severe pitting attack; the samples were immersed for 20 min in 0.04 M KSCN solutions without and with $5x10^{-3}$ M Gly at 25 ºC. Measurements were performed under potentiostatic regime at 1400 mV (anodic to the pitting potential, E_{pit}, recorded for Al in 0.04 M KSCN), and finally washed thoroughly and submitted for 20 min to ultrasonic cleaning in order to remove loosely adsorbed ions. The morphology of the passive layer and the corrosion products formed on the electrode surface were again examined by EDX and SEM examinations.

Results and discussion

Chemical studies

ICP-AES measurements

The open-circuit free corrosion rate was determined separately, using ICP-AES technique, by determination of dissolved Al^{3+} ions in aerated 0.04 M KSCN solutions without and with various concentrations (10^{-5} – $5x10^{-3}$ M) of Gly at 25 ^{o}C. In the course of ICP experiments, localized corrosion is not supposed to be formed. Otherwise, the results cannot be compared with those obtained from the linear polarization technique (see later). This is because linear polarization measures only the uniform corrosion rate, particularly when it is performed at potentials around the corrosion potential (E_{corr}), i.e., within the potential range of Tafel region. Indeed, after 30 days of immersion, no pits were observed under the optical microscope (100 × magnification). Thus, extensive pitting attack does not exist. The absence of pitting attack under these conditions was further confirmed here, as will be seen, using SEM.
In the ICP experiments, known aliquots of the solution containing dissolved Al^{3+} ions were withdrawn as a function of time and Gly concentration and were analyzed to produce the corrosion-time curves depicted in Fig. 1. The slope of each line (mass, in mg, of Al dissolved as Al^{3+} per unit area per unit time; mg cm^{-2} h^{-1}) represents the corrosion rate of Al at the specified conditions. The numerical values of these slopes were converted into the corresponding corrosion current density values using Faraday's law, and subsequently converted into

corrosion rates, $\upsilon_{ICP\text{-}AES}$, in μm y^{-1} (Micrometer per year; the penetration rate of corrosion through a metal) using the expression [31]:

$$\upsilon_{ICP\text{-}AES}\ (\mu m\ y^{-1}) = 3280 \times j_{corr} \times (M / nd) \quad (1)$$

where M is the atomic weight of Al (26.98154 g), n the number of electrons transferred in the corrosion reaction (n = 3) and d the density of Al (2.70 g cm^{-3}). As the corrosion rate depends directly on mass of Al dissolved, the addition of Gly results in a decrease in this parameter. This is clearly seen from the decrease of the mass of dissolved Al with Gly concentration. These findings indicate that Gly can be considered as inhibitor of Al uniform corrosion in KSCN solutions.

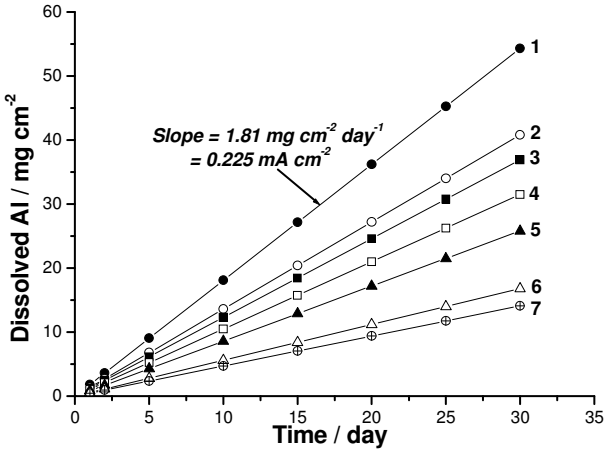

Figure 1. Corrosion-time plots recorded for Al in aerated 0.04 M KSCN solutions without and with various concentrations (10^{-5} – 5×10^{-3} M) of Gly at 25 °C.
(1) blank; (2) 10^{-5} M Gly; (3) 5×10^{-5} M Gly; (4) 10^{-4} M Gly; (5) 5×10^{-4} M Gly; (6) 10^{-3} M Gly; (7) 5×10^{-3} M Gly.

The corrosion currents obtained from the ICP method were also used to evaluate inhibition efficiency values, $I_{ICP\text{-}AES}(\%)$, as a function of Gly concentration, using the well-known expression:

$$I_{ICP\text{-}AES}(\%) = 100 \times [(j^{o}_{corr} - j_{corr}) / j^{o}_{corr}] \quad (2)$$

where j^{o}_{corr} and j_{corr} are the corrosion current densities for uninhibited and inhibited solutions, respectively. Fig. 2 shows the corrosion rates ($\upsilon_{ICP\text{-}AES}$) and inhibition efficiencies ($I_{ICP\text{-}AES}$ (%)) as a function of Gly concentration at 25 °C. It follows from Fig. 2 that the corrosion rate is suppressed, and therefore the corrosion inhibition strengthened, with increase in Gly concentration. This trend may result from, as will be shown soon, the fact that adsorption and surface coverage increases with the increase in inhibitor concentration; thus the surface is separated from the medium [32].

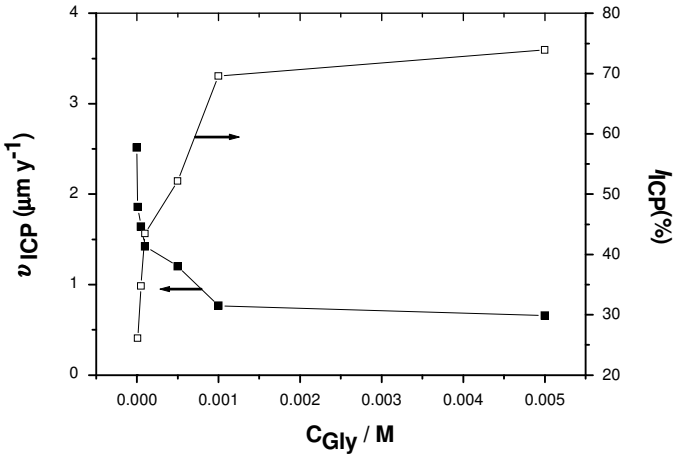

Figure 2. Corrosion rates ($\upsilon_{ICP\text{-}AES}$) against inhibition efficiencies ($I_{ICP\text{-}AES}$ (%)), obtained from ICP-AES method of chemical analysis, for Al in aerated 0.04 M KSCN solutions without and with various concentrations (10^{-5} – 5×10^{-3} M) of Gly at 25 °C.

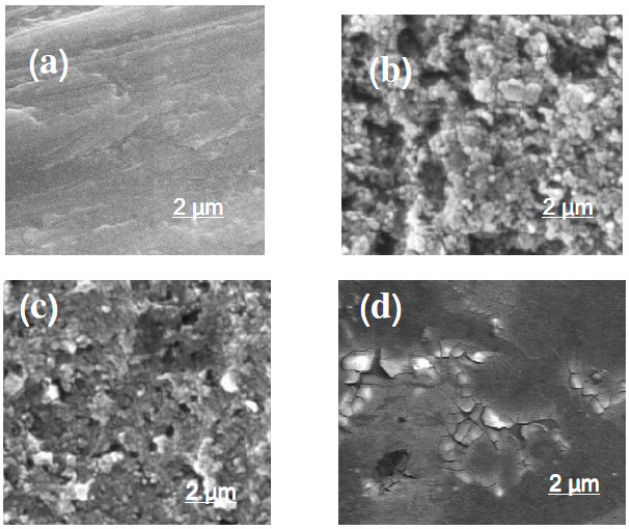

Figure 3. SEM images obtained for **(a)** polished Al, and for Al, after a full immersion test of 30 days at 25 °C, in aerated 0.04 M KSCN solution without (image b) and with $5x10^{-4}$ M Gly (image c), or with $5x10^{-3}$ M Gly (image d) at 25 °C.

A surface film of Gly is assumed to be formed, protecting Al against uniform corrosion in SCN^- solutions. This was confirmed from surface analysis (SEM and EDX examinations) performed for the corroded and inhibited Al samples, see Figs. 3 and 4. Regarding to the SEM images presented in Fig. 3, the mechanically polished Al electrode without any treatment (clean sample, image a) shows that the Al sample immersed in 0.04 M KSCN solution has corrosion areas on its polished surface (see image b) which do not exist on the clean sample. The appearance of such corroded areas may be attributed to the dissolution of alumina layer due to the aggressive attack of SCN^- anions and the increased alkalinity of the solution in the vicinity of the electrode surface (see more details in section 3.2.2).

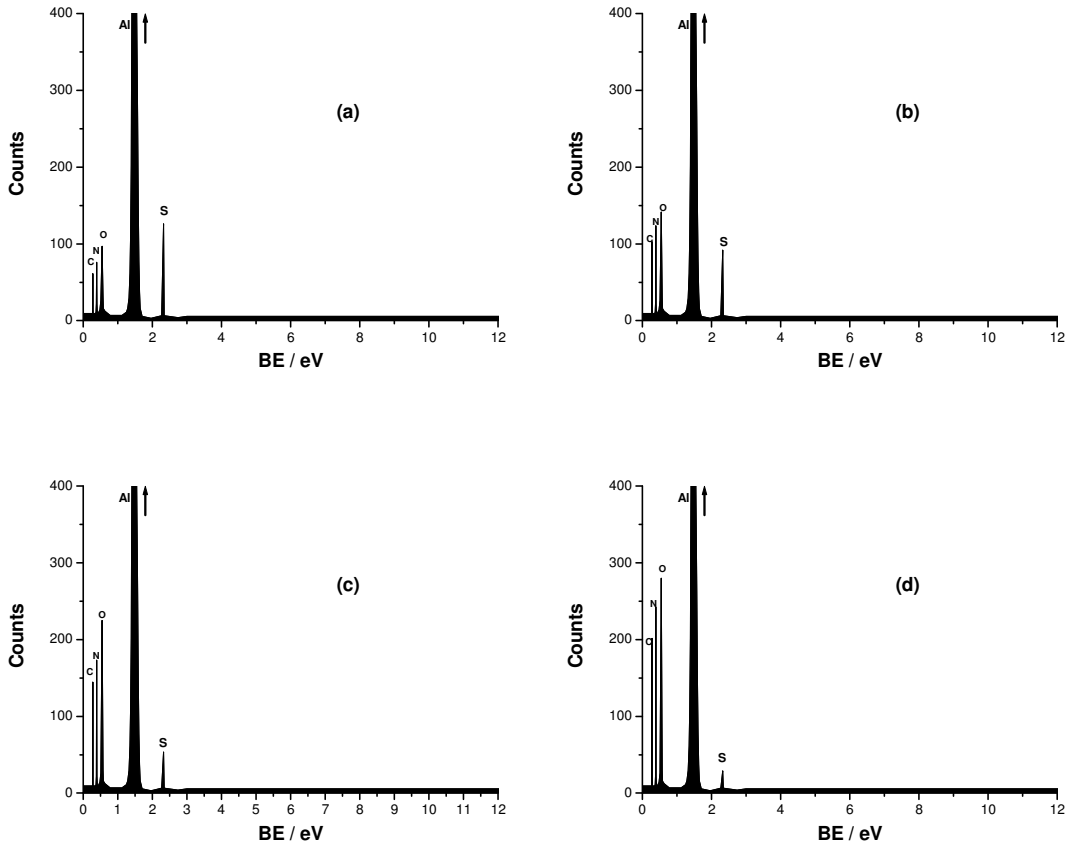

Figure 4. EDX spectra recorded for Al, after a full immersion test of 30 days at 25 ^{o}C, in aerated 0.04 M KSCN solution **(a)** without and **(b)** with 5×10^{-4} M Gly, **(c)** 10^{-3} M Gly**,** or **(d)** 5×10^{-3} M Gly at 25 ^{o}C.

On the other hand, in presence of Gly, there is an improvement in the surface morphology due to the obvious decrease in the corroded areas caused by the Gly layer covering the active sites. This improvement in the surface morphology enhances with Gly concentration (images c-d). Therefore, it can be concluded that on the Al surface, after a full immersion test of 30 days in aerated 0.04 M KSCN solutions containing various concentrations of Gly, a protective film of the inhibitor is developed, and the protectiveness of such film depends on Gly concentration.

On the other hand, the EDX spectra of Fig. 4 contain peaks characteristic of C, N and S in the passive Al_2O_3 film (characterized by Al and O signals). The presence of C, N and S signals reflects the adsorption and incorporation of the aggressive SCN^- anions onto the passive oxide film [8]. In presence of Gly, the contribution of signals of C, N and O obviously enhances, as a function of Gly concentration (see Figs. 4b-d), at the expense of the S signal compared with their contribution in bare KSCN solution (Fig. 4a).

Thus, considering the EDX analysis, it can be concluded that the main action of Gly is to impede the adsorption of SCN^- anions and the dissolution of the oxide film to an extent depending on Gly concentration. As a consequence, the alumina layer is protected against corrosion.

All previous results reveal that the corrosion inhibition effect of Gly is due to its adsorption onto the aluminum surface blocking the corrosion process. Two types of mechanisms of inhibitor adsorption may be considered. The first is physical (electrostatic) adsorption, the most probable one, and the second may be chemical adsorption assisted by hydrogen bond formation between inhibitor and the oxidized electrode surface (see more details in section 4).

Electrochemical measurements

OCP vs. time curves

As mentoned in the experimental part, special care was taken in the stability of the OCP before each polarization run. Moreover, measuring the variation with time of the OCP of the working electrode is important in defining domains of corrosion, partial and complete inhibition, and in determining inhibitor-threshold concentrations [33]. Fig. 5 illustrates the evolution of the open circuit potential (OCP) with immersion time of Al in an aerated solution of 0.04 M KSCN in the absence or in the presence of various concentrations of Gly at 25 ^{o}C.

In the absence of Gly (curve 1), it can be seen, in first moments of the period of immersion, how the corrosion potential moves rapidly towards less negative values due to the formation of the oxide layer. Then, the electrode potential shifts rapidly towards the more negative values during the first 20 min of immersion. This evolution may be attributed to the adsorption of SCN^- anions, confirmed from EDX examinations of the electrode surface at the open circuit potential (see Fig. 4a). For increasing immersion times, the open circuit potential goes towards a more positive value and keeps a constant value (steady potential) after about 90 min of immersion due to the formation of a porous layer of alumina [34]. This steady potential corresponds to the free corrosion potential, E_{corr}, confirmed from polarization studies (section 3.2.2) of the metal; similar results were previously obtained [35].

Bockris [34] has shown that the passive layers on aluminium involve a porous pre-layer of $Al(OH)_3$ and Al_2O_3. Part of the Al_2O_3 is AlO(OH), in fibril form. Destruction of the passive layer involves penetration of these fibrils by Cl^-, which displaces the passivating species and diffuses out in the form of an $AlCl_n^{m+}$ complex. In agreement with [34] as well as our previous study [8], SCN^- anions are expected to behave like Cl^-, with the subsequent formation of $Al(SCN)_3$ soluble species.

On the other hand, upon introducing Gly, new curve features were recorded, depending on Gly concentration. Addition of dilute concentrations of Gly (curves 2-5 in Fig. 3a) or GlyD (curves 2 and 3 in Fig. 4a), for the first moment of immersion, shifts significantly the electrode potential to more negative values in comparison with the solution without inhibitor (curve 1). The magnitude of this negative shift of potential depends on the concentration of the tested inhibitor. At the same time, the growth of the oxide film is slowed down due to the decrease in the slope of the initial linear part of E vs. t plots. In addition, the steady state E_{corr} drifts to more negative values without changing the general shape of the OCP vs. time plots. This negative shift in E_{corr} enhances with increase in Gly concentration.

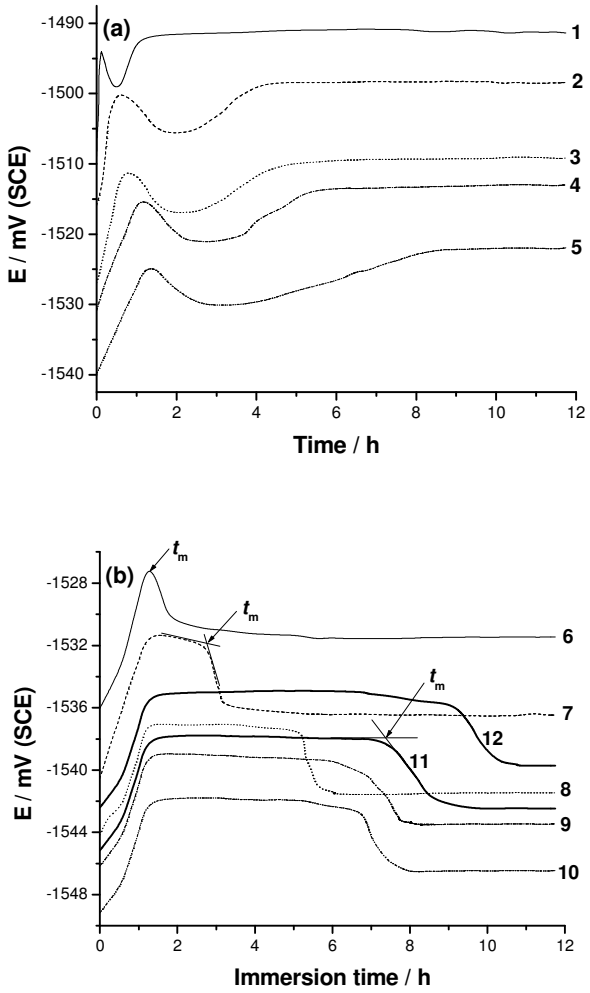

Figure 5. Open circuit potential vs. time plots recorded for Al in aerated 0.04 M KSCN solutions without and with various concentrations of Gly at 25 ^{o}C.

For concentrations of Gly higher than 7.5×10^{-5} M (Fig. 5b, curves 6-10), the OCP shifted first to less negative values reaching a maximum. After a certain time, depending on inhibitor concentration, the potential declined to a reasonably steady value. This trend indicated the occurrence of two counter-acting processes. The first process being the formation of a protective layer of the inhibitor on the electrode surface, and consequently delayed-action corrosion occurred shifting the OCP to nobler values. The second process is corrosion, due to adsorption of the aggressive SCN^- anions, which dragged the potential back towards active values. This means that a competitive adsorption exists between the inhibitor, as will be seen, and the aggressive SCN^- anions.

This competition may explain the appearance of an arrest in the corresponding OCP vs. time curves. The time corresponding to the end of this arrest, see again Fig. 5b, is designated here as t_m. It is obvious that the parameter t_m is dependent upon the Gly concentration. Values of t_m are always longer in presence of increasing concentrations of Gly. These findings, as a first sight, indicate that Gly

inhibits, confirming results of ICP, Al corrosion in SCN^- solutions to an extent depending on its concentration. Thus, surface coverage, and therefore inhibition performance of Gly increases with increase in its concentrations.
However, the appearance of this arrest indicates that Gly under these conditions is not able to ensure effective corrosion inhibition. The progressive negative shift in E_{corr} with increasing Gly concentration (inspect again Fig. 5) may be explained on the basis that Gly adsorbs preferentially on the electrode surface, impeding the cathodic sites (see more details in section 3.2.2). At $C_{Gly} > 10^{-3}$ M, see curves 11 and 12 in Fig. 5b, the OCP shifted to less negative values, reaching a reasonably steady value. These findings may also reflect the ability of Gly to inhibit the anodic process too.

Polarization measurements
Inhibition of uniform corrosion
Fig. 6 shows the cathodic and anodic polarization plots recorded for Al in 0.04 M KSCN solution without and with various concentrations of Gly at a scan rate of 0.5 mV s^{-1} at 25 ^oC. Regarding to region I, the increase in Gly concentration reduced both the anodic and cathodic current densities and shifted the corrosion potentials (E_{corr}) to more negative values. These results indicate that Gly possesses a stronger influence on retarding the electrochemical processes occurring on the cathodic sites of Al surface, more than on the anodic sites (dissolution of Al). This means that Gly may be classified as a mixed-type inhibitor that acts predominately on the cathodic sites.
The anodic process that takes place on the electrode surface is Al dissolution as a result of the reaction presented in Eq. 3:

$$Al \leftrightarrows Al^{3+} + 3e^- \quad (3)$$

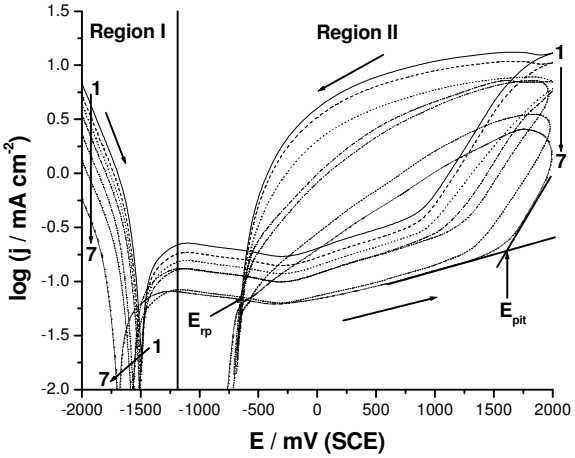

Figure 6. Cyclic polarization curves recorded for Al in aerated 0.04 M KSCN solutions without and with various concentrations (10^{-5} – 10^{-3} M) of Gly at a scan rate of 0.5 mV s^{-1} at 25 ^oC. (1) blank; (2) 10^{-5} M Gly; (3) 5×10^{-5} M Gly; (4) 10^{-4} M Gly; (5) 5×10^{-4} M Gly; (6) 10^{-3} M Gly; (7) 5×10^{-3} M Gly.

The associated cathodic response is that of reduction of dissolved O_2 and/or H_2O, as indicated in reactions (4) and (5):

$$2H_2O + 2e^- \leftrightarrows H_2\uparrow + 2OH^- \quad (4)$$

$$O_2 + 2H_2O + 2e^- \leftrightarrows 4OH^- \quad (5)$$

As a result of these reactions, the local pH becomes more alkaline; hence the layer of aluminum oxide is dissolved according to the reaction:

$$Al_2O_3 + 2OH^-_{ads} \leftrightarrows 2AlO_2^-{}_{(aq)} + H_2O \quad (6)$$

In parallel, Al oxidation by uniform corrosion may occur, and a layer of aluminum oxide is formed, with the physical detachment of gaseous hydrogen, according to reaction (7):

$$2Al + 3H_2O \leftrightarrows Al_2O_3 + H_2\uparrow \quad (7)$$

Extrapolation of Tafel lines is one of the most popular DC techniques for estimation of corrosion rate. Polarization plots presented in Fig. 6 (region I) allow us to estimate the corrosion current density (j_{corr}) from Tafel extrapolation of the cathodic curves to E_{corr}. All the recorded j_{corr} values were introduced in Eqs. 1 and 2 to obtain the corrosion rate, υ_{Tafel}, and inhibition efficiency, $I_{Tafel}(\%)$, values, as a function of Gly concentration (Fig. 7). A decrease in the corrosion rate, corresponding to an increase in the inhibition efficiency, can be clearly noticed. These results parallel those recorded in Fig. 2 coming from the ICP method of chemical analysis.

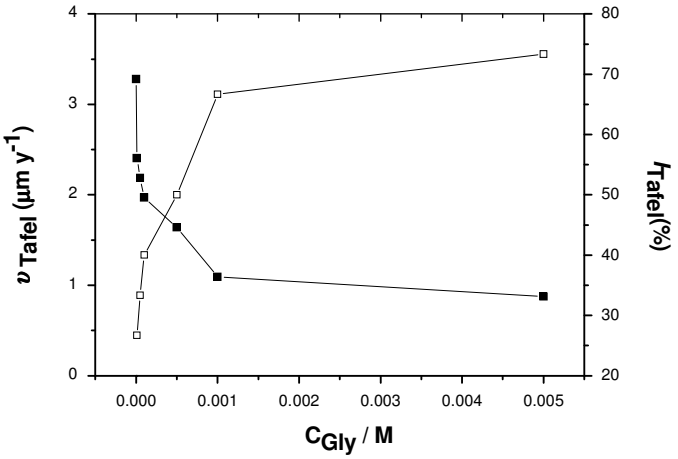

Figure 7. Corrosion rates (υ_{Tafel}) against inhibition efficiencies (I_{Tafel} (%), obtained from polarization measurements, for Al in aerated 0.04 M KSCN solutions without and with various concentrations (10^{-5} – 5×10^{-3} M) of Gly at 25 °C.

Inhibition of pitting corrosion

It was also the purpose of the present work to determine the inhibition power of Gly against pitting corrosion of Al in the aggressive SCN^- solutions. To achieve this, the anodic behavior of Al regarding corrosion, passivation and breakdown of passivity in these solutions was studied, move to region II in Fig. 6.

It is obvious that Al pits in KSCN solutions exhibiting a well-defined hysteresis loop, characteristic of passivation breakdown on the upward sweep and repassivation. The existence of a hysteresis loop in a cyclic potentiodynamic polarization curve indicates that repassivation of an existing pit is more difficult when the potential is scanned toward the negative direction.

The larger the hysteresis loop, the more difficult the repassivation is. E_{pit} represents the potential limit above which the formation of pitting begins. E_{rp} refers to the limit below which the metal remains passive, and it is defined as the potential where the forward and reverse scan cross; it marks the division between stable and unstable passivity. Intermediate values between E_{pit} and E_{rp} did not permit the formation of new pits, but allowed the development of those which already existed. The narrower the hysteresis loop the easier it becomes to repassivate the pit.

Based on the above argument, cyclic polarization technique is therefore useful in determining the degree of protection against pitting corrosion provided by Gly as well as its effect on the characteristics steps of this form of localized attack, i.e., nucleation of new pits and growth of pre-existing pits. According to [9], two factors should contribute to the overall pitting corrosion resistance. First, the resistance against the nucleation of new pits and, secondly, a growth resistance of pre-existing pits. The former has been evaluated as the difference, R, between the pitting potential, E_{pit}, and the corrosion potential, E_{corr}. Though this R parameter cannot be used in absolute terms, it is very useful when used as a comparative parameter. Thus, a higher R value refers to a higher resistance against pit nucleation.

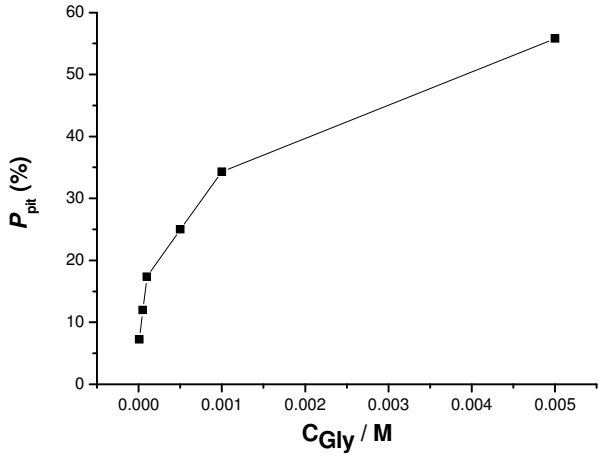

Figure 8. Estimated values of the degree of protection against pitting nucleation, P_{pit}, as a function of Gly concentration at 25 ^oC.

The protection degree against pitting nucleation, designated here as P_{pit}, was therefore estimated in terms of the percentage increase of parameter R. The reference value of this parameter, i.e., R^o, was taken in the cyclic polarization experiment carried out in bare KSCN solution. Fig. 8 shows the degree of protection against pitting nucleation, P_{pit}, as a function of Gly concentration. Fig. 8 reveals that P_{pit} increases with increase in Gly concentration.

The resistance against growth of pre-existing pits was evaluated by comparing the areas of the anodic hysteresis loops observed in the cyclic polarization diagrams plotted in the j/E style, not included here. Using a specific routine of the M352 Corrosion Software, the areas of the anodic hysteresis loops were calculated. This area is related to the electrochemical charge consumed during the growth of the pre-existing pits. The percentage decrease of this area, from the value observed for the blank solution, was taken as a measure for the protection degree against pitting growth. From these values the percentage decrease of spent power, P_g, can be calculated (see Fig. 9).

The P_g parameter can be used as a measurement of the resistance against pitting growth. From Figs. 8 and 9, addition of Gly to aggressive SCN^- solutions resulted in an improved behaviour against pitting corrosion of Al. However, the protection efficiency against uniform and pitting corrosion processes still unsatisfied, see Figs. 2 and 12, and requires much improvement. This being one aspect that undoubtedly deserves further study.

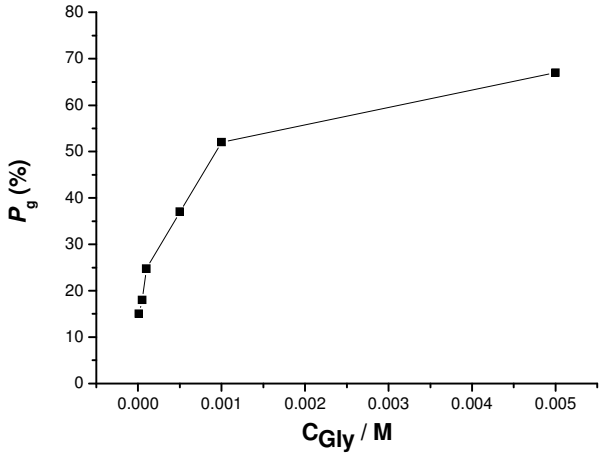

Figure 9. Degree of protection values, $P_g(\%)$, against pit growth as a function of Gly concentration at 25 °C.

Surface analysis (Figs. 10 and 11) also revealed the adsorption and the subsequent inhibition power of Gly against pitting corrosion of Al in aggressive SCN^- solutions. Surface morphologies presented in Fig. 10 revealed the occurrence of intense pitting corrosion on the specimen exposed to this high anodic potential (positive to E_{pit}). A large pit can be observed with an average diameter close to 50 μm. This large pit was apparently composed of several smaller pits and some pits were formed at the bottom of previous formed pits.

The radial growth of this large pit seems to begin by the coalescence of small pits. It seems that the rate of radial growth of large pits as well as their penetration rate is high and observable at this high applied anodic potential, yielding intense pitting attack. In contrast to this, little pitting attack is observed in the SEM image of the sample tested, under the same experimental conditions, in Gly-SCN^--containing solutions, see Fig. 10.

The EDX spectra depicted in Fig. 11, performed for the two samples that were previously prepared for the SEM examinations (Fig. 10), gave exactly the same trend of the EDX spectra presented in Fig. 4. Just note the high contribution of C, N and S signals in Fig. 11 compared with their contribution in Fig. 4. This was attributed, as reported in our previous study [8], to the applied anodic potential effect. Here again, the adsorption and incorporation of Gly was confirmed. These results suggest that Gly can also play an important role as a pitting corrosion inhibitor.

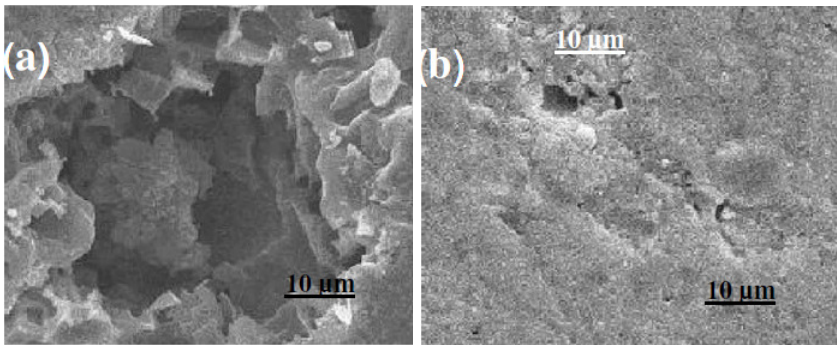

Figure 10. SEM images obtained for Al subjected to severe pitting attack in aerated 0.04 M KSCN solutions without (image a) and with (image b) 5×10^{-3} M Gly. Severe pitting conditions (the sample is potentiostatically held at 1300 mV, > E_{pit}, for 30 min) at 25 ^{o}C.

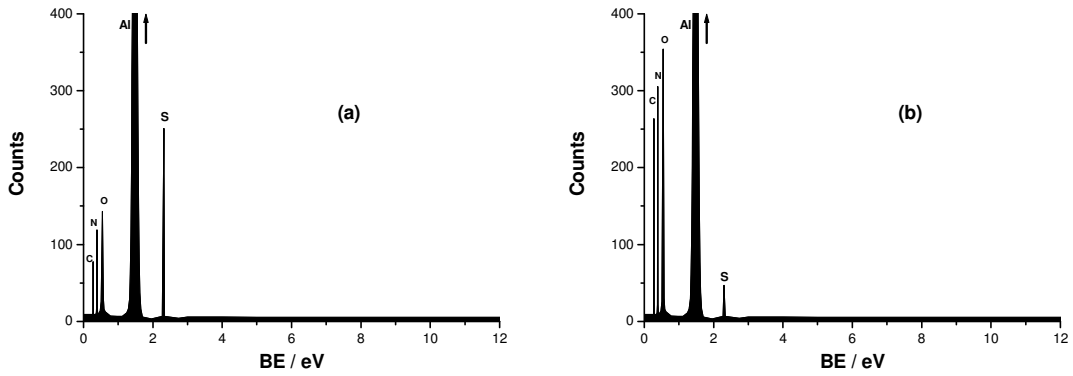

Figure 11. EDX spectra obtained for Al subjected to severe pitting attack, as described in Fig. 7, in aerated 0.04 M KSCN solutions (a) without and (b) with 10^{-3} M Gly at 25 ^{o}C.

Mechanism of inhibition

It is well-known that the phenomenon of adsorption is influenced by the nature and surface charge of the metal and by the chemical structure of inhibitors. Terminal oxygen atoms at metal oxide surfaces react with water, forming hydroxylated sites that impart a pH-dependent surface charge. Surface charge depends on activities of potential-determining ions (H^+ and OH^-) and electrolyte concentrations (ionic strength, I) [36]. The pH where the net total particle charge is zero is called the point of zero charge (PZC). The point of zero charge is an important parameter characterizing the adsorption properties of metal oxides and related materials [37,38].

The pH of the PZC for aluminum oxides/hydroxides is 9 [39,40]. Depending on the solution pH, the electrode surface can bear net negative, or positive, or no charge. In 0.04 M KSCN solution (pH 6.8), therefore oxide surface is positively charged. This positive charge of the electrode surface at E_{corr} was further confirmed via defining the position of E_{corr} with respect to the respective PZC ($E_{q=0}$) [41-43]. When the difference u = [(E_{corr} − $E_{q=0}$ = 0) is negative, the electrode surface acquires a negative net charge and the adsorption of cations is favoured. On the contrary, the adsorption of anions is favoured when u becomes positive.

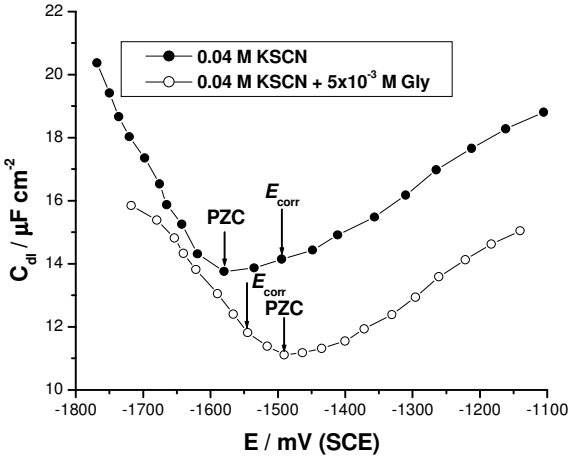

Figure 12. The C_{dl} vs. *E* plot recorded for Al in 0.04 M KSCN solution (a) without and (b) with 5×10^{-3} M Gly.

It has been shown in the literature that ac impedance studies can be used to evaluate the PZC from the capacitance (C_{dl}) versus applied potential (*E*) plot [41-43, 44]. Fig. 12 represents the variation of C_{dl} with *E* recorded for Al in 0.04 M KSCN solution in the absence (curve 1) and presence (curve 2) of $5x10^{-3}$ M Gly. The minima on the C_{dl} versus *E* curves are considered as the value of PZC of the electrode. It is obvious from Fig. 12 that the surface charge of Al in KSCN solutions at the free corrosion potential is positive (u = [−(1495) − (−1580) = + 85 mV(SCE)]).

In absence of Gly, this positive charge of the oxide film may favour the electrostatic adsorption of the aggressive SCN^- anions. The adsorbed SCN^- anions may cooperate, as previously mentioned, with the increased alkalinity of

the solutions (due to reactions 4 and 5) to dissolve and damage the passive layer (inspect again the SEM image presented in Fig. 3b).

Regarding to Fig. 12, Al surface carries positive excess charge in 0.04 M KSCN solutions (curve 1), whereas negative excess charge is carried on the Al surface in the presence of Gly (curve 2), (u = [−(1550) − (−1490) = − 60 mV(SCE)]). These results indicate that when adding Gly to KSCN solution, Gly molecules (with its positive center, namely the protonated amino group) quickly adsorb electrostatically at the oxide/solution interface through electrostatic attraction force because of the excess negative charge (due to the adsorbed layer of the SCN^- anions) at this interface at the corrosion potential. Due to this electrostatic adsorption, part of the positive charges on the metal surface is shielded. It is not surprising now to understand why the PZC is shifted positively in presence of Gly (see again curve 2 in Fig. 12). This adsorption of Gly impedes further adsorption of the aggressive SCN^- anions (inspect again the EDX spectra presented in Figs. 4 and 11). Thus the electrode is protected against corrosion.

In addition to this physical (electrostatic) adsorption, there should be chemisorption assisted by hydrogen bonding. This H-bond may be formed between the protonated N–H linkages in the Gly structure and the oxygen atoms of the passive film. This type of adsorption is expected to be effective, because the positive charge on the N-atom is conductive to the formation of hydrogen bonds. However, this type of adsorption requires sensitive surface analysis, like FT-IR and XPS, to be confirmed. This being one aspect that deserves further investigation.

It seems that the adsorbed layer of Gly is not well-protective; it may be porous, cracked or something else: inspect again SEM images presented in Figs. 3 and 10. In addition, the S signal (due to the adsorption of aggressive SCN^- anion) is still visible in the EDX spectra, even at high concentrations of Gly (see Figs. 4 and 11). This means that the Gly layer is not protective enough to completely prevent the adsorption of SCN^- anions.

These findings confirm the results obtained from the OCP vs. time plots (Fig. 5) that Gly, under the operating conditions, is not enough to ensure permanent-corrosion inhibition. This is the reason why a new Gly derivative is synthesized in our lab in order to effectively inhibit the corrosion of Al in the aggressive SCN^- solutions. Promising results were obtained with this new Gly derivative and will be presented in a full separate paper.

Conclusion

This work reports results of ICP-AES method of chemical analysis, Tafel polarization and cyclic polarization on the ability of glycine (Gly) to inhibit uniform and pitting corrosion processes of Al in aerated non-stirred 0.04 M KSCN solutions at 25 ^oC. These studies have shown that Gly is able to inhibit uniform and pitting corrosion of Al in KSCN solutions, as indicated by the decrease in the corrosion current and the increase in the pitting potential. Inhibition efficiency is a function of Gly concentration. The inhibition by Gly is proposed to be due to the formation of a Gly adsorbed film on the metal surface

that protects the metal against the aggressive attack of SCN^- anions. Scanning electron microscopy (SEM) and energy dispersion X-ray (EDX) observations of the electrode surface confirmed the existence of such an adsorbed film.

References

1. G.A. Capauano, W.G. Davenport, *J. Electrochem. Soc.* 118 (1971) 1688. 10.1007/BF00620581
2. P. Fellener, M.C. Paucivova, K. Mataisovsky, *Surf. Technol.* 14 (1981) 101.
3. C.-C. Yang, *Mater. Chem. Phys.* 37 (1994) 355. 10.1016/0254-0584(94)90175-9
4. M.A. Amin, S.S. Abd El-Rehim, E.E.F. El-Sherbini, *Electrochim. Acta* 51 (2006) 4754. 10.1016/j.electacta.2006.01.015
5. M.A. Amin, S.S. Abd El-Rehim, S.O. Moussa, A.S. Ellithy, *Electrochim. Acta* 53 (2008) 5644. 10.1016/j.electacta.2008.03.010
6. M.A. Amin, H.H. Hassan, O.A. Hazzazi, M.M. Qhatani, *J. Appl. Electrochem.* 38 (2008) 1589. 10.1007/s10800-008-9600-9
7. M.A. Amin, *Electrochim. Acta* 54 (2009) 1857. 10.1016/j.electacta.2008.10.009
8. M.A. Amin, S.S. Abd El Rehim, E.E.F. El-Sherbini, S.R. Mahmoud, M.N. Abbas, *Electrochim. Acta* 54 (2009) 4288. 10.1016/j.electacta.2009.02.076
9. S. Szklarska-Smialowska, *Pitting Corrosion of Metals* D. 296. NACE, Houston, Texas (1986).
10. M. Koudelkova, J. Augustynski, M. Berthou, *J. Electrochem. Soc.* 124 (1977) 1165. 10.1149/1.2133520
11. J.S. Wainright, O.J. Murphy and M.R. Antonio, *Corros. Sci.* 33 (1992) 281. 10.1016/0010-938X(92)90152-S
12. C.M.A. Brett, I.A.R. Gomes and J.P.S. Martins, *J. Appl. Electrochem.* 24 (1994) 1158. 10.1007/BF00241315
13. C.M.A. Brett, I.A.R. Gomes, J.P.S. Martins, *Corros. Sci.* 36 (1994) 915. 10.1016/0010-938X(94)90194-5
14. S.S. Abdel Rehim, H.H. Hassan, M.A. Amin, *Appl. Surf. Sci*. 187 (2002) 279. 10.1016/S0169-4332(01)01042-X
15. A.A. El-Shafei, S.A. Abd El-Maksoud, A.S. Fouda, *Corros. Sci*. 46 (2004) 579. 10.1016/S0010-938X(03)00067-2
16. A.K. Maayta, N.A.F. Al-Rawashdeh, *Corros. Sci*. 46 (2004) 1129. 10.1016/j.corsci.2003.09.009
17. QiBo Zhang, YiXin Hua, *Mat. Chem. Phys*. 119 (2010) 57. 10.1016/j.matchemphys.2009.07.035
18. I.B. Obot, N.O. Obi-Egbedi, S.A. Umoren, *Corros. Sci*. 51 (2009) 276. 10.1016/j.corsci.2008.11.013
19. Nabel A. Negm, Mohamed F. Zaki, *Colloids and Surfaces A: Physicochem. Eng. Aspects* 322 (2008) 97. 10.1016/j.colsurfa.2008.02.027
20. K.R. Baldwin, M.C. Gibson, P.L. Lane and C.J.E. Smith, Proceedings of the 7th European Symposium on Corrosion Inhibitors (7 SEIC), Ann. Univ. Ferrara, N.S. SEZ V. Suppl. 9 (1990) 711.
21. M. Metikos-Hukovic, R. Babic, Z. Grubac, S. Brinic, *J. Appl. Electrochem.* 24 (1994) 772. 10.1007/BF00578093
22. M.A. Amin, S.S. Abd EI-Rehim, E.E.F. El-Sherbini, O.A. Hazzazi, M.N. Abbas, *Corros. Sci*. 51 (2009) 658. 10.1016/j.corsci.2008.12.008

23. S.S. Abd El Rehim, H.H. Hassan, M.A. Amin, *Corros. Sci*. 46 (2004) 5. 10.1016/S0010-938X(03)00133-1
24. M.A. Amin, Q. Mohsen, Omar A. Hazzazi, *Mat. Chem. Phys*. 114 (2009) 908. 10.1016/j.matchemphys.2008.10.057
25. S.S. Abd El Rehim, M.A. Amin, S.O. Moussa, A.S. Ellithy, *Mat. Chem. Phys*. 112 (2008) 898. 10.1016/j.matchemphys.2008.06.039
26. S.S. Abd El Rehim, H.H. Hassan, M.A. Amin, *Mat. Chem. Phys*. 78 (2003) 337. 10.1016/S0254-0584(01)00602-2
27. S.S. Abd El Rehim, H.H. Hassan, M.A. Amin, *Mat. Chem. Phys*. 70 (2001) 64. 10.1016/S0254-0584(00)00468-5
28. M.A. Amin, *J. Appl. Electrochem*. 39 (2009) 689. 10.1007/s10800-008-9710-4
29. K.F. Khaled, M.A. Amin, *J. Appl. Electrochem.* 39 (2009) 2553. 10.1007/s10800-009-9951-x
30. ASTM G 31, Standard Practice for Laboratory Immersion Corrosion Testing of Metals, Licensed for BASF, p.5.
31. Electrochemistry and Corrosion-Overview and Techniques, Application Note CORR-4, EG and G, Princeton Applied Research, USA.
32. T. Zhao, G. Mu, *Corros. Sci.* 41 (1999) 1937. 10.1016/S0010-938X(99)00029-3
33. A.M. Shams El Din, R.A. Mohammed, H.H. Haggag, *Desalination* 114 (1997) 85. 10.1016/S0011-9164(97)00157-4
34. J. O'M. Bockris, Lj. V. Minevski, *J. Electroanal. Chem.* 349 (1993) 375. 10.1016/0022-0728(93)80186-L
35. L. Garrigues, N. Pebere, F. Dabosi, *Electrochim. Acta* 41 (1996) 1209. 10.1016/0013-4686(95)00472-6
36. H. van Olphen, An Introduction to Clay Colloid Chemistry, 2nd ed., Interscience Publications, New York (1977).
37. F.I. Morais, A.L. Page, L.J. Lund, *Soil Sci. Soc. Am. J.* 40 (1976) 521.
38. G.A. Parks, P.L. de Bruyn, The zero point of charge of oxides, *J. Phys. Chem.* 66 (1961) 967. 10.1021/j100812a002
39. H. Hohl, M. Stumm, *J. Colloid Int. Sci.* 55 (1976) 281. 10.1016/0021-9797(76)90035-7
40. R.Wood, D. Fornasiero, J. Ralston, *Colloids Surf.* 51 (1990) 389. 10.1016/0166-6622(90)80154-V
41. M.A. Amin, *J. Appl. Electrochem.* 36 (2006) 215. 10.1007/s10800-005-9055-1
42. H.H. Hassan, E. Abdelghani, M.A. Amin, *Electrochim Acta* 52 (2007) 6359. 10.1016/j.electacta.2007.04.046
43. M.A. Amin, S.S. Abd El-Rehim, E.F.E. El-Sherbini, R.S. Bayoumi, *Electrochim. Acta* 52 (2007) 3588. 10.1016/j.electacta.2006.10.019
44. A. Lukomska, J. Sobkowski, *J. Electroanal. Chem*. 567 (2004) 95. 10.1016/j.jelechem.2003.11.063